# Supplementary Material for "Early Warning of mmWave Signal Blockage Using Diffraction Properties and Machine Learning"

Amirhassan Fallah Dizche, *Student Member, IEEE,* Alexandra Duel-Hallen, *Fellow, IEEE,* and Hans Hallen

In this supplementary document, we provide additional numerical results and derivations that are referred to in the paper.

## S1. Simple Model Derivation

In this section, we present the derivation of the simple model discussed in Section II of the paper. This simple model is used to provide insights into the Fresnel calculation results. As noted in the main text, the simple model consists of the interference between the direct LoS beam from the transmitter and a cylindrical wave from the blocker's edge. We defined there the distance $d$ between the blocker edge and the receiver path where the path crosses the geometric LoS/NLoS transition (see Fig. 1). The angle $\alpha$ away from normal of the path crossing is also shown in Fig. 1. Let $s$denote a scalar distance along the path from LoS $(x_0, y_0)$ to NLoS $(x_1, y_1)$ with zero value at the geometric transition; it is negative in the LoS region, positive in NLoS.

The realistic physical model is based upon the coordinates $(x, y)$ as shown in Fig. 1, but these are not optimal for deriving the simple model. Instead, we create a set of coordinates $(u, q)$ by translating $(x, y)$ so that the origin is at the blocker edge $\mathbf{r}_{bl}$, then rotate so that the coordinate $u$ is along the geometric transition from the blocker as shown in Fig. 1. The coordinate $q$ is perpendicular to $u$ and also measured from the blocker but towards LoS. The distance from the $(u, q)$ origin, $\mathbf{r}_{bl}$, to the mobile is $r = \sqrt{u^2 + q^2}$ (see Fig. 1). The interference between the two waves $h_T$ and $h_{edge}$ is given by the sum of the direct signal traveling along $u$ and the cylindrical wave traveling along $r$. The cylindrical wave amplitude scales as $1/\sqrt{r}$. We also include a phase factor $\phi$ to account for the response of the scattering. The direct plane wave has amplitude $A$, and the amplitude of the cylindrical wave is thus $A_e = A\sqrt{d}$. Then the passband received signal corresponding to (2) is given by

$$\begin{aligned}\tilde{h}(u, v) =& A\,cos(\omega t - ku) + A\sqrt{d/r}\,cos(\omega t - kr + \phi)\\ =& A\,[cos(\omega t)\,cos(ku) + sin(\omega t)\,sin(ku)+\\ &+ \sqrt{d/r}\,cos(\omega t)\,cos(ku + \phi)+\\ &+ \sqrt{d/r}\,sin(\omega t)\,sin(ku + \phi)]\\ =& A\,cos(\omega t)\,[cos(ku) + \sqrt{d/r}\,cos(kr + \phi)]+\\ &+ A\,sin(\omega t)\,[sin(ku) + \sqrt{d/r}\,sin(kr + \phi)].\end{aligned}$$

This work was partially supported by National Science Foundation Grant ECCS-2122012.

From the above, the squared envelope of the equivalent lowpass signal is given by

$$\begin{aligned}h^2 =& A^2/2\,[cos^2(ku) + d/r\,cos^2(kr + \phi)+\\ &+ 2\sqrt{d/r}\,cos(ku)cos(kr + \phi) + sin^2(ku)+\\ &+ d/r\,sin^2(kr + \phi) + 2\sqrt{d/r}\,sin(ku)sin(kr + \phi)]\\ =& A^2/2\,[1 + d/r + \sqrt{d/r}\,cos(ku - kr - \phi)]\\ =& A^2/2\,[1 + d/r - \sqrt{d/r}\,cos(ku - kr)],\end{aligned}$$

where the last line assumes that $\phi = 180^\circ$ as expected and is consistent with the known result of $h^2 = A^2/2$ along the geometric transition where $u = d = r$. This result is placed onto the path of the mobile in the LoS region (where $s$ is negative),

$$\begin{aligned}u &= d - s\,sin(\alpha);\;\; q = -s\,cos(\alpha)\\ r &= \sqrt{d^2 - 2ds\,sin(\alpha) + s^2 sin^2(\alpha) + s^2 cos^2(\alpha)}\\ &= \sqrt{d^2 + s^2 - 2ds\,sin(\alpha)}.\end{aligned}$$

To convert to (2), we rewrite the mobile path parameter $s$ as $s = -v(t - t_t)$ where here the speed is $v$ and referenced to a time $t_t$ when the UE crosses the geometric transition. Inserting this into the above, we obtain (2) in the paper, but with $u$ and $r$ time-dependent via substituting for $s$: $u = d - v(t - t_t)\,sin(\alpha)$ and $r = \sqrt{d^2 + v^2(t - t_t)^2 - 2dv(t - t_t)\,sin(\alpha)}$.

Furthermore, as we note in the paper, the simple model fails in the NLoS region and its envelope variation is not correct in the LoS region. This is expected due to its simplicity, so we do not use it for any training or testing scenario creation (the realistic physical model is used for those cases). It does, however, capture the correct trends for variation of $d$, $\alpha$ and $f_c$. Results in Fig. S1 can be compared to the Figs. 3(b-c) in the main text. Thus, the simple model is useful for insights into the origins of several key properties of the pattern used for early warning.

## S2. Effect of the Dataset $\mathcal{D}$ size $N$

To study the effect of size of the dataset $\mathcal{D}$ on EW performance, in section III-B of the paper, second paragraph, we vary $N$ from 1000 to $100,000$ and report the EW accuracy, f1 score, and AUC for each case. Table S1 summarizes the simulation results. We observe that for $N < 10,000$ the EW performance degrades while increasing $N$ over $10,000$ does not change the EW performance significantly. Therefore,

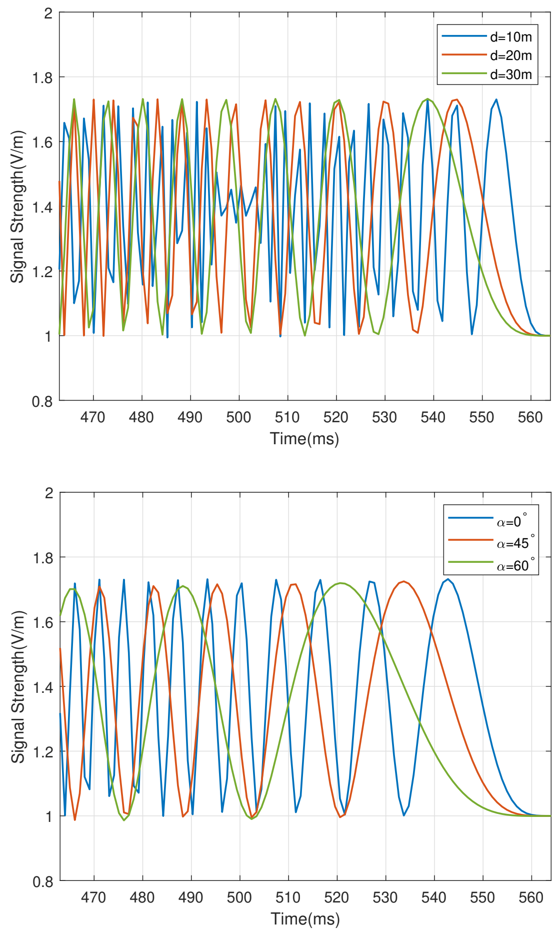


(a)

(b)

Fig. S1. Parameter variation calculations of the simple model for a 5 m path length ending at the geometric transition $s = 0$ with speed 28 m/s, the $T_x$ at (x, y) = (-10, 0) m and the blocker at (0, 0) m so the (x, y) and (u, q) axes are the same. (a) Change $d$: $\alpha_1 = \alpha_2 = \alpha_3 = 0°; d_1 = 50m, d_2 = 30m, d_3 = 10m$. Compare to Fig. 3-b. (b) Change $\alpha$: $\alpha_1 = 0°, \alpha_2 = 45°, \alpha_3 = 60°; d_1 = d_2 = d_3 = 40m$. Compare to Fig. 3-c.

$N = 10,000$ is a suitable size for dataset $\mathcal{D}$. In S3, S2, similar conclusions were reached for other prediction times $t_s$, $P$, and noise variance $\sigma^2$.

TABLE S1
EW PERFORMANCE VS DATASET SIZE $N$, $W = 400(ms)$, $f_s = 1$KHZ, $t_1 = 250(ms)$, $P = 50(ms)$, NOISELESS DATA.

| $N$ | Accuracy | f1 score | AUC |
|---|---|---|---|
| 1000 | 89.74% | 0.8259 | 0.8712 |
| 3000 | 97.87% | 0.9641 | 0.9641 |
| 6000 | 98.86% | 0.9793 | 0.9839 |
| 10000 | 99.53% | 0.9919 | 0.9955 |
| 20000 | 99.60% | 0.9928 | 0.9972 |
| 100000 | 99.61% | 0.9928 | 0.9972 |

## S3. Effect of Speed on Early Warning

As discussed in Section IV, paragraph 2, speed has negligible effect on early warning (EW) performance. Table S2 illustrates these results.

TABLE S2
EW PERFORMANCE VS UE AND BLOCKER SPEED, $W = 400(ms)$, $f_s = 1$KHZ, $t_1 = 250(ms)$, $P = 50(ms)$.

| UE & Blocker speed | Accuracy | f1 score | AUC |
|---|---|---|---|
| $0 - 5(m/s)$ | 99.93% | 0.9989 | 0.9947 |
| $5 - 10(m/s)$ | 99.78% | 0.9940 | 0.9918 |
| $10 - 15(m/s)$ | 99.67% | 0.9933 | 0.9901 |
| $15 - 20(m/s)$ | 99.53% | 0.9901 | 0.9854 |
| $20 - 25(m/s)$ | 99.41% | 0.9883 | 0.9834 |
| $25 - 30(m/s)$ | 99.37% | 0.9855 | 0.9820 |

## S4. Performance metrics for noisy measurements

Additional simulation for the f1 score and AUC of the experiments described in the last paragraph of Section IV in the paper are provided in the following figures.

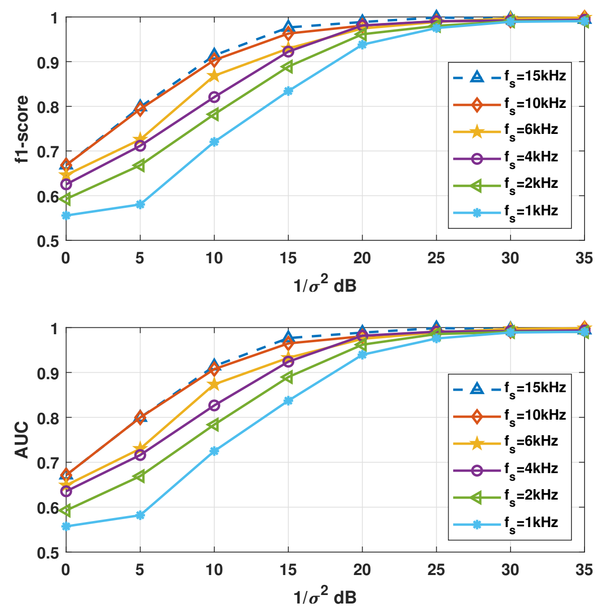


Fig. S2. F1 score and AUC of mmWave EW of blockage vs $1/\sigma^2$ for $f_s = \{1, 2, 4, 6, 10, 15\}$ kHz, $W = 400(ms)$, $t_1 = 250(ms)$ and $P = 50(ms)$. See Fig. 6 in the paper.